minerals

MDPI

Article

Clay Schists from Barrancos (Portugal): An Approach Toward Sustainable Ceramic Raw Material Use

Carla Candeias *, Sónia Novo and Fernando Rocha

GeoBioTec Research Unit, Geosciences Department, University of Aveiro, Campus de Santiago, 3810-193 Aveiro, Portugal

* Correspondence: candeias@ua.pt

Abstract

This study presents a comprehensive mineralogical, chemical, and technological characterization of clay schist samples from Barrancos (southern Portugal), aiming to evaluate their suitability for sustainable ceramic production. The work integrated X-ray diffraction (XRD), X-ray fluorescence (XRF), thermal analysis (TGA, DTA, and dilatometry), and other assays. After simple dry milling, the clay schist samples' texture supported their use in plastic ceramic pastes but indicated a need for blending with coarser materials to meet extrusion requirements. Mineralogical analysis confirmed a dominance of illite (82%–85%), with minor kaolinite and chlorite. Chemical composition revealed significant Al_2O_3 (21.65%–28.24%) and SiO_2 (52.27%–58.99%) contents, while Fe_2O_3 (4.41%–8.89%) supported their use in red ceramics. The presence of K_2O (up to 5.43%) and Na_2O (up to 1.63%) contribute to the fluxing capacity, promoting vitrification. Cation exchange capacity and specific surface area were low, consistent with the mineralogy dominated by illite and kaolinite. Thermal analysis confirmed the formation of mullite after firing at 1100 and 1150 °C, alongside residual quartz and hematite. The ceramic bodies exhibited progressive densification and strength enhancement with increasing temperature. The mixture of two selected samples showed good mechanical properties and lower porosity, with no efflorescence observed. These results underscore the potential of these schists as sustainable raw materials for ceramic production, promoting regional economic valorization and reducing environmental impact by utilizing local resources.

Keywords: clay schist; geo resources; ceramics; sustainability; barrancos

check for updates

Academic Editor: Janos Kristof

Received: 12 June 2025
Revised: 24 July 2025
Accepted: 7 August 2025
Published: 11 August 2025

Citation: Candeias, C.; Novo, S.; Rocha, F. Clay Schists from Barrancos (Portugal): An Approach Toward Sustainable Ceramic Raw Material Use. *Minerals* **2025**, *15*, 852. https://doi.org/10.3390/min15080852

Copyright: © 2025 by the authors. Licensee MDPI, Basel, Switzerland. This article is an open access article distributed under the terms and conditions of the Creative Commons Attribution (CC BY) license (https://creativecommons.org/licenses/by/4.0/).

1. Introduction

Clay-based materials are among the most important natural resources used in the production of ceramics worldwide. Their broad availability, low cost, and inherent plasticity make them key components in the manufacture of bricks, roofing tiles, floor tiles, and structural ceramics. Globally, ceramic production exceeds 30 billion m^2/year, with raw materials such as clay schists, kaolinite, and illite playing vital roles in these industrial processes [1]. The selection and development of alternative clay sources with suitable mineralogical and technological properties are increasingly critical to ensure sustainable production amid growing environmental concerns. Several studies have emphasized the valorization of alternative clay resources, such as clay schists, for industrial ceramics. These materials are commonly found in sedimentary or low-grade metamorphic formations and are characterized by layered textures and a predominance of phyllosilicates [2]. The technological potential has been explored in several countries, including Spain, Italy, and

Morocco, where schists have been successfully integrated into ceramic manufacturing [3,4]. The drive for circular economy solutions and the reduction in extraction pressure on traditional clay deposits further reinforces the importance of evaluating underutilized materials like clay schists.

In Portugal, the ceramic sector plays a vital role in the national economy, contributing notably to exports and regional employment. The Alentejo region, in particular, has a long-standing tradition of ceramic production and is currently focused on adopting sustainable strategies to remain competitive while minimizing its environmental impact. The use of local raw materials, such as clay-rich schists of the Barrancos area, presents a promising path to support this objective. The valorization of these materials not only diversifies raw material sources but also promotes the circular use of natural resources that are often disregarded as low-value geotechnical waste [5]. The present study focuses on the mineralogical and technological assessment of clay schists from the Barrancos Formation in southeastern Portugal. When appropriately processed and fired, the compositional characteristics and mechanical behavior meet the standards required for structural ceramics. The economic context of Barrancos further enhances the relevance of this research. As a rural municipality with limited industrial diversification, the valorization of local georesources for ceramic applications can stimulate job creation, promote sustainable development, and attract investment. Furthermore, the use of dry milling processes and low-impact forming and firing techniques aligns with international sustainability goals and European Union directives targeting resource efficiency and emission reduction in manufacturing [6,7].

This study aims to assess the suitability of Barrancos clay schists for structural ceramics by analyzing the mineralogical, chemical, granulometric, and technological properties, both individually and as mixed raw materials. Through a comprehensive series of laboratorial assays, including thermogravimetric, dilatometric, and mechanical tests, this work evaluated the potential for red ceramic production under sustainable and economically viable conditions. While the use of illite- and kaolinite-rich clays in ceramics is well-documented, the contribution of this study lies in the first detailed validation of these specific local resources for red ceramic production. Despite being previously mapped geologically, the Barrancos clay schists had not been systematically characterized for ceramic applications. This new data can help safeguard raw material continuity for nearby industries that are increasingly affected by the depletion of conventional clay deposits. Beyond the local context, this research has broader relevance: in a global setting marked by rising transportation costs, energy insecurity, and material scarcity, the identification of local alternatives to imported raw materials supports the transition toward more resilient, circular, and low-carbon manufacturing systems. This aligns with global sustainability agendas that promote resource autonomy, reduced environmental impact, and regional development. Accordingly, this study makes a relevant scientific and strategic contribution to both ceramic materials science and the broader effort to enhance the resilience of raw-material-intensive industries.

2. Materials and Methods

2.1. Sampling Location and Geological Context

The clay schists were collected at a quarry, located in Barrancos (Portugal), at coordinates 38°3′35.13″ N 7°28′38.52″ W (Figure 1). At the quarry, schist blocks are extracted and, by their natural cleavage planes, separated into pieces to be used in construction, particularly for paving and cladding. Geologically, the study area belongs to the Ossa-Morena Zone (OMZ), one of the major paleogeographic units of the Iberian Peninsula. The samples were collected from the unit corresponding to the Barrancos Formation (lower Ordovician), with a thickness reaching ~800 m in this area [8]. Its upper level is composed of greenish-gray micaceous schists with millimetric detrital lamination. These schists typically

exhibit abundant meandriform bioturbation structures, especially at the studied quarry, where extensive bedding surfaces are covered with trace fossils [9]. In the down section, the sequence transitions into purple-violet micaceous schists interbedded with gray schists. At the base, violet schists predominate, intercalated with meter-thick layers of greenish, fine-grained, micaceous schists, exhibiting millimetric siltstone laminations. The purple schists of Barrancos are reminiscent of "wine-dreg" schists, commonly associated with volcanic environments. However, no clear connection with volcanic rocks was evident in the Barrancos region, and the coloration is likely controlled by the depositional environment, possibly oxidizing [10]. The sampled clay schists were oriented NW–SE from the upper section of the Barrancos Formation. At the quarry, these schists are exploited on the NE flank (inverted) of an anticline structure, bounded to the NE and SW by Silurian formations. The exploited layers displayed an average attitude of NW–SE, dipping ~70° SW, closely corresponding with bedding planes. The quarry exhibits jointing in directions NE–SW (85° SE) and E–W (~75° S), along with some zones of crushed rock. In the upper part, layers were weathered and imbricated [8]. Along schistosity planes, dark manganese and iron-rich dendritic infillings were occasionally observed.

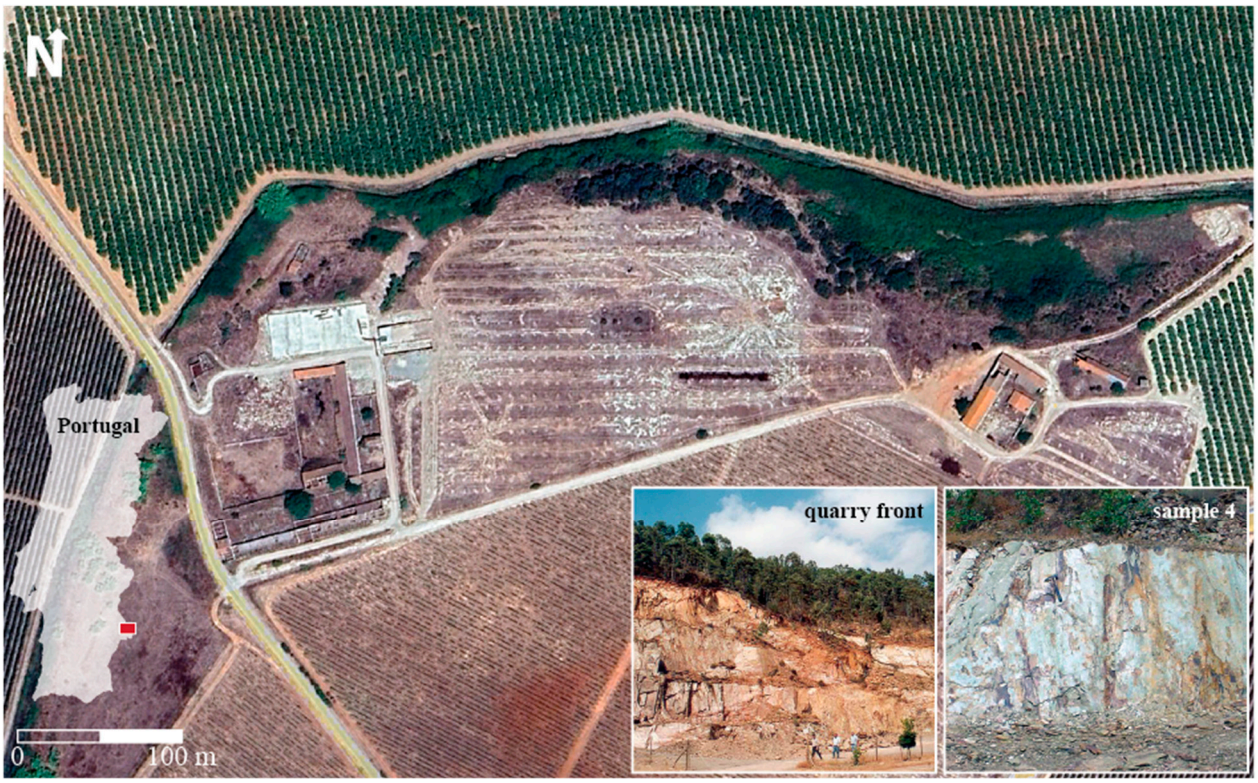


Figure 1. Satellite image, location of the quarry on the map of Portugal (red rectangle), and images of quarry front (with people for scale), and sample 4 location (with a rock hammer for scale). Adap. Google Earth Pro® and [11].

For this study, four samples (two from core drillings and two from the quarry front) were collected on the selected quarry: sample 1, from the base of an 18 m deep borehole; sample 2, from the base of a 16 m deep borehole; sample 3, from the quarry front, being representative of the overall lithology; and sample 4, collected from the quarry front, but with a noticeably different appearance (whitish, silky, and pearly) clearly distinguishing it from the general characteristics of the outcrop (Figure 1).

2.2. Methodology

Clay schist samples were subjected to mechanical fragmentation due to their high consistency. A portion of each sample was retained as a reference before processing. The samples were then oven-dried at 40 °C to prevent mineralogical alteration. Subsequently, the material was quartered and milled in an agate mill for 10 min at 700 rpm. X-ray fluorescence (XRF) was performed on the grounded samples, oxides Al_2O_3, CaO, Fe_2O_3, K_2O, MgO, MnO, Na_2O, P_2O_5, SiO_2, and TiO_2, and trace elements As, Ba, Cr, Cu, Nb, Ni, Pb, Rb, Sr, V, Zn, and Zr, respectively. A Panalytical Axios PW4400/40 (Malvern Panalytical, Malvern, Worcestershire, UK) was used with Rh radiation. Loss of ignition (LOI) was assessed by calcination on a muffle at 1000 °C for 3 h. To determine the concentrations of Na_2O and K_2O, a flame photometer Corning, model 400 (Corning Medical & Scientific Ltd, Halstead, Essex, UK) was used. By X-ray diffraction (XRD), mineral phases were identified, using a Philips/Panalytical powder diffractometer (Malvern Panalytical, Malvern, Worcestershire, UK), model X' Pert Pro MPD, with a Cu-X-ray tube operated at 50 kV and 30 mA, data collected from 2 to 70° 2θ with a step size of 0.01° and a counting interval of 0.02 s [5]. After diffractogram interpretation, the relative abundance of each mineral phase was semi-quantitatively estimated based on the reflection intensities using the peak area method [12]. Illite crystallinity (IC) was determined using the Kübler index. The pH was determined using a sample–water solution in a 1:2.5 ratio, using a WTW Microprocessor pH Meter 537 (Wissenschaftlich-Technische Werkstätten GmbH, Weilheim, Germany) [13].

Cation exchange capacity (CEC) and the concentrations of the main exchangeable cations (Ca^{2+}, Mg^{2+}, Na^+, and K^+, and total Fe) were determined using a saturating solution of ammonium acetate (1 M and pH 7), followed by displacement of the adsorbed ammonium ions with KCl, and quantified after by atomic absorption spectroscopy (AAS) [11]. The expandability of sample materials was analyzed following standard LNEC E200-67 [14]. The plasticity index (PI) and plastic (PL) and liquid (LL) limits were evaluated following the Atterberg limits [15], using the expression PI = LL − PL [5]. Specific surface area (SSA) was measured using the BET (Brunauer–Emmett–Teller) method, using Gemini II 2370 equipment (Micromeritics® Instrument Corporation, Norcross, GA, USA) [16]. Operating conditions for thermogravimetric analysis (TGA) and differential scanning calorimetry (DSC) were identical, as the thermograms were recorded simultaneously to assess thermal analysis (STA) with a Netzsch STA 449 C thermobalance, equipped with a TASC 414/3A temperature control system [17,18]. The heating rate was set to 10 °C/min up to 1000 °C using a sample mass of ~20 mg. Thermodilatometric (TD) analysis was performed according to standard DIN 51045-1949 [19].

For the forming process, the extrusion method [20] was selected using a mixture of samples 2 and 3, which revealed similar characteristics in the previous assays. Extrusion was carried out using a Netzsch 250/05 extruder (Netzsch Group, Selb, Germany) equipped with a vacuum capacity of 0.85 Pa. The drying process was carried out to determine ceramic properties before firing, where test specimens were subjected to mechanical and thermal stresses, along with deformations that can lead to the development of tensile and/or shear cracks. Linear shrinkage was measured on dried specimens using a caliper [21], and flexural strength (FS) of the dried specimens was determined in accordance with standard ASTM C689-97 (green) [22], using a LLOYD Instruments testing machine (Lloyd Instruments Ltd, Bognor Regis, West Sussex, UK) with a loading rate of 1 N/s. Firing tests, on extruded and dried specimens, were conducted at 900 °C, 1000 °C, and 1100 °C, using a Termolab electric chamber furnace, with a heating rate of 5 °C/min and a soaking time of 60 min at the target temperature. Temperatures of 1000 °C and 1100 °C were selected based on established industrial practices for red ceramics, such as bricks and roofing tiles, where sintering, densification, and vitrification typically occur within this range.

These values are consistent with guidelines from standards like EN 1304 (clay roofing tiles) [23] and EN 771-1 (clay masonry units) [24] and reflect common firing regimes used in energy-efficient roller kilns. This range also enables the evaluation of critical ceramic transformations, including mullite formation and the evolution of technological properties such as shrinkage, mechanical strength, and water absorption, ensuring the relevance of the results for industrial applications. Mineralogical changes that occurred after firing were studied by XRD on representative portions of each specimen fired at different temperatures, in both the outer and inner parts. Water absorption (WA) capacity was determined in the fired specimens by immersion in water, boiling for two hours, and cooling for four hours. After removing excess surface water, specimens were weighed and dried in an oven at 110 °C for 24 h and weighed again, WA being the relative percentage of the different weights. Efflorescence tests were conducted on fired specimens after flexural strength by being placed in a tray with deionized water reaching halfway up their height and left to rest for 24 h, then dried in an oven at 110 °C for 24 h and assessed semi-quantitatively for the presence of efflorescence. The color of the fired bodies at different temperatures was also visually assessed.

3. Results and Discussion

The clay schist samples were subjected to dry milling in an agate mill to assess the granulometric distribution, revealing a predominance of fine fractions, with the <0.063 mm fraction representing over 95% of the total mass in all samples (Figure 2). The clay-sized fraction (<0.002 mm) ranged from 23.9 to 43.8%, while the coarse fraction (>0.063 mm) was minimal (0.1 to 4.9%). In fact, the D50 showed that >50% of the particles in the samples were sized 0.0038 (1), 0.0046 (2), 0.0057 (3), and 0.0025 mm (4). Results indicated that a simple dry milling procedure can be both effective and selective. It produced materials with granulometric characteristics consistent with those required for ceramic shaping and sintering, particularly in plastic ceramic pastes. This laboratory-scale dry processing approach aligns with current trends in the ceramic industry, aiming to reduce the environmental impact and costs. Compared to conventional wet milling, dry preparation methods have demonstrated significant reductions in water (74% less) and energy consumption (36% less electrical and 78% less thermal energy) [6]. Additionally, CO_2 direct emissions are also lower when using the dry method as opposed to the wet method due to the reduction in thermal energy obtained from natural gas combustion (76% less). Given the favorable granulometric profile obtained, the studied schist materials showed good potential for use in ceramic formulations, especially in sustainable production routes.

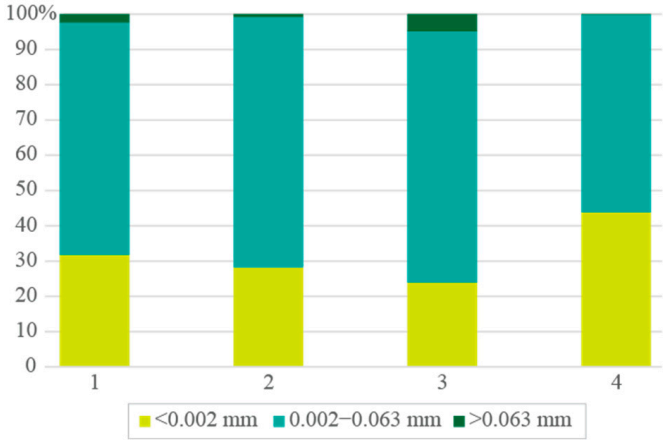


Figure 2. Clay schist samples' granulometry, after simple dry milling.

The granulometric composition of the four clay schist samples was plotted on the Winkler diagram (Figure 3), commonly used to assess the suitability of clay raw materials for specific ceramic products. According to this classification system, defined fields correspond to typical uses: (I) common bricks, (II) perforated bricks, (III) roofing tiles and masonry bricks, and (IV) hollow brick wall and pavement [4,25]. All studied samples were plotted outside the defined suitability zones of the diagram, suggesting that, based on the particle size distribution after simple milling, samples do not meet the granulometric requirements for traditional ceramic product extrusion. Specifically, the dominance of the 0.002–0.020 mm fraction and the low content of coarse particles (>0.063 mm) led to marginal placement within the Winkler diagram fields, indicating potential challenges in plasticity and shaping behavior during forming. This outcome is comparable to observations reported by Hmeid et al. [4] in a study of clays from northeastern Morocco, where some smectite-rich materials also fell outside the extrusion-favorable areas of the Winkler diagram. The high clay and silt fractions led to very high plasticity but needed blending with coarser materials to reduce cracking and improve handling during forming. The Barrancos samples, therefore, highlighted the need for technological adjustments, namely, particle size optimization or blending with less plastic materials, to ensure workability and extrusion potential.

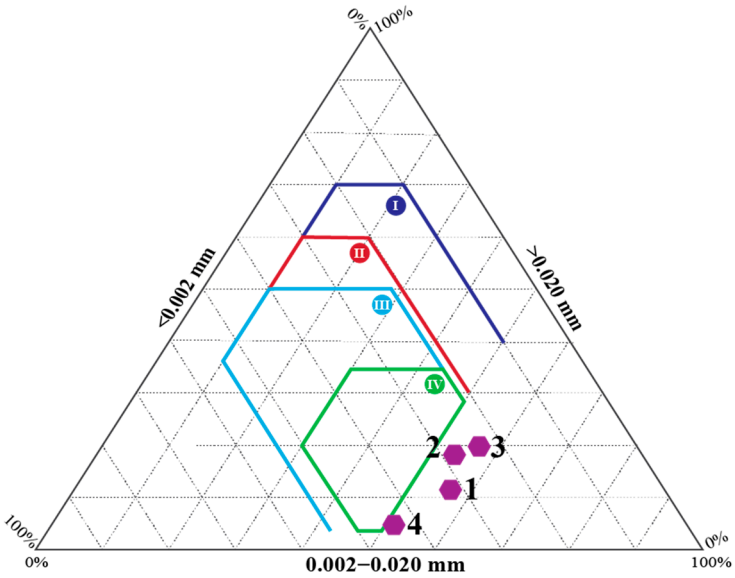


Figure 3. Clay schist samples, 1 to 4, projected in the Winkler diagram, with suitable fractions for ceramic manufacturing: zone I—solid bricks; zone II—perforated bricks; zone III—roofing tiles and masonry bricks; and zone IV—hollow brick wall and pavement [4,25].

The dominant mineral phases identified in the four samples were phyllosilicates (29%–37%), quartz (14%–20%; SiO_2), and K and Na feldspars, with minor amounts of dolomite ($CaMg(CO_3)_2$), anhydrite ($CaSO_4$), and siderite ($FeCO_3$) (Table 1). Phyllosilicates are particularly relevant in ceramic formulations, contributing to plasticity and green mechanical strength [26]. Quartz acts as a non-plastic filler, being essential for dimensional stability and shrinkage control during drying and firing. Although high quartz content can increase brittleness in green bodies, the sample content remains within acceptable ranges for structural ceramic bodies [3]. K-feldspar and plagioclase present in similar proportions function as fluxing agents, promoting vitrification and mechanical strength after firing by facilitating the formation of liquid phases above 1000 °C [27]. While 7% dolomite is moderate, its fine dispersion within the clay matrix ensures that CO_2 evolution during thermal decomposition (~700–900 °C) creates internal pore spaces and moderate densification. Experiments with cream-firing clays showed that even minor dolomite

additions can affect porosity and physical properties [28], suggesting that 7% dolomite can influence porosity and act as a secondary flux in ceramic firing. This controlled presence may enhance thermal behavior without significantly compromising mechanical performance. Opal C/CT (2%–9%) and anhydrite (4%–5%) are indicative of diagenetic transformations and sulfate content, respectively. While anhydrite may contribute to bloating and SO_2 emissions if present in high amounts, its consistent but moderate presence ($\leq$5%) suggested controllable behavior during firing [29]. Siderite (up to 11%) and traces of hematite (Fe_2O_3) and pyrite (FeS_2), Fe-bearing phases, may influence the final coloration of the ceramic products, particularly under oxidizing kiln atmospheres, where Fe-oxides typically promote red to reddish-brown hues [30]. Identified mineral phases reflected a promising composition for structural ceramic production, especially for materials requiring moderate plasticity and sufficient fluxing action. Nevertheless, the high phyllosilicate and carbonate content, in combination with the granulometric profile, reinforces the idea that blending with coarser or less plastic materials may be necessary to optimize performance in extrusion and firing processes. These clay schists showed potential to be incorporated into sustainable ceramic production chains, aligning with current environmental and resource efficiency goals in the ceramic industry [7].

Table 1. Identified mineral phases in the clay schist samples (in %; tr—trace; ——not detected).

Mineral	1	2	3	4
Quartz	20	14	17	14
Phyllosilicates	32	31	29	37
K-feldspar	12	12	12	14
Plagioclase	17	16	13	13
Calcite	tr	1	1	–
Dolomite	7	7	7	7
Opal C/CT	2	2	9	4
Anhydrite	4	5	5	5
Siderite	5	11	5	5
Pyrite	–	1	tr	–
Hematite	1	1	1	tr

The mineralogical analysis of the clay fraction revealed a strong predominance of illite (82%–85%) in the four samples (Figure 4). Illite ($K_{0.65}Al_2[Al_{0.65}Si_{3.35}O_{10}](OH)_2$) is a non-expandable, mica-type clay mineral that significantly contributes to the moderate plasticity, thermal stability, and mechanical strength of the ceramic bodies during firing [31]. This mineral's prevalence suggested that these materials are suitable for structural ceramics such as bricks and tiles. Kaolinite ($Al_2(Si_2O_5)(OH)_4$) content varied between 9 and 12%, providing additional plasticity and green body strength while contributing to a more stable shrinkage profile upon drying and firing. Kaolinite's dihydroxylation at ~500–600 °C also facilitates early vitrification, which may be beneficial for energy-efficient ceramic production [32]. Chlorite, present in minor but consistent amounts (2%–5%), may play a secondary role. While chlorite decomposes between 550 and 700 °C, releasing volatiles such as H_2O and Mg/Fe-rich gases, its limited presence is not expected to significantly affect ceramic performance. However, it may contribute to color variation or influence porosity development during firing [33]. The dominance of illite, with secondary kaolinite and minor chlorite, suggested that the clay fraction was rich in non-expanding, thermally stable phyllosilicates, a favorable mineralogical composition for red ceramic production. These features, combined with the previously described granulometric profile and accessory mineralogy, reinforce the potential of these clay schists for integration into industrial ceramic formulations, particularly in sustainable, low-impact production chains.

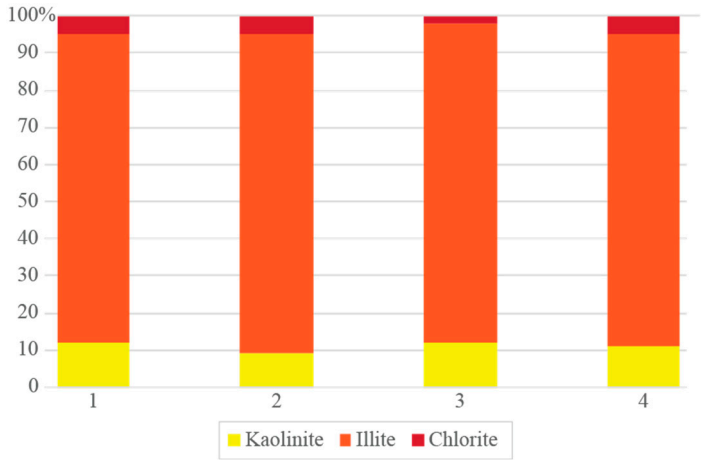


Figure 4. Relative distribution of the identified mineral phases in the <0.002 mm fraction of the clay schist samples.

The results of the illite crystallinity analysis indicated low Kübler index values, indicative of a certain degree of structural order [34]. A narrower illite peak width corresponds to more advanced diagenesis, which enhances the crystalline ordering of the mineral. The I(002)/I(001) ratio in all clay schist samples was high, exceeding 0.3, suggesting the presence of aluminous illites of the muscovite type. According to Gomes [35], the Esquevin index revealed that the clay schist samples exhibited compositions close to phengite, except for sample 4, compositionally closer to muscovite. All four samples fell within the diagenetic-to-low-grade metamorphic transition zone (anchizone). The position of the samples in the anchizone field was supported by the low values of the 10 Å peak full width at half maximum, indicating high illite crystallinity. Moreover, the Al/(Fe + Mg) ratio was highest in sample 4, consistent with the chemical composition, with lower Fe_2O_3 and MgO content, and higher Al_2O_3 content (Table 2). The high crystallinity of illite observed in all samples, particularly the aluminous character and compositional maturity, can be favorable for structural ceramic applications [36]. Crystalline illites contribute to moderate plasticity, enhance the mechanical strength of the green body, and provide stability during drying and firing. The predominance of phengitic and muscovitic illites, with limited interlayer expansion, minimizes the risk of shrinkage-related defects and favors dimensional stability. Additionally, the lower Fe and Mg content in sample 4 suggested less potential for undesirable color development or bloating during firing, making it particularly suitable for products where color uniformity or whiteness is valued. Overall, the crystallinity and chemical maturity of illite in these clay schists supported the technological suitability for sustainable ceramic production, especially in the manufacture of bricks, roofing tiles, or stoneware bodies.

Table 2. Oxide composition of the clay schist samples (in %; LOI—loss of ignition).

ID	Al_2O_3	CaO	Fe_2O_3	K_2O	MgO	MnO	Na_2O	P_2O_5	SiO_2	TiO_2	LOI
1	21.65	0.09	6.10	3.92	1.10	0.23	1.63	0.13	58.99	1.13	4.33
2	22.28	0.08	6.74	3.70	1.25	0.16	1.44	0.14	58.77	1.16	4.14
3	22.80	0.05	8.89	4.05	1.04	0.12	1.19	0.18	55.37	1.14	5.05
4	28.24	0.04	4.41	5.43	0.80	0.02	1.52	0.15	52.27	1.33	5.61

The chemical analysis revealed that all samples exhibited high SiO_2 (52.27 to 58.99%) and Al_2O_3 (21.65 to 28.24%) content, consistent with the quartz and phyllosilicate minerals present. The high alumina values reflected the abundance of illite and kaolinite, reinforcing the plastic and refractory properties of the clay matrix. Sample 4, different from the

others, showed the highest alumina content, aligned with its thinner granulometric profile and illite present. The Fe_2O_3 content ranged from 4.41 to 8.89%, typical of red-firing clays used in ceramic production [1]. The Fe-oxides act as coloring agents, promoting reddish to brown hues under oxidizing conditions [29]. The highest Fe_2O_3 content was recorded in sample 3, expected to influence the fired color intensity of ceramic bodies derived from this material. Alkaline (Na_2O 1.19%–1.63%) and alkaline-earth oxides (K_2O 3.70%–5.43%) were present in relevant proportions. These oxides are natural fluxing agents, promoting vitrification and the development of liquid phases above 1000 °C. The relatively high K_2O content, particularly in sample 4, can be advantageous for enhancing mechanical strength post-firing due to the formation of feldspathic glassy phases [1]. The MgO (0.80%–1.25%) and CaO (0.04%–0.09%) contents were relatively low, minimizing the risk of excessive bloating or expansion during firing. The presence of MnO and TiO_2 in trace amounts may slightly influence coloration and melting behavior but is not expected to compromise ceramic performance [37]. The P_2O_5 content was low, suggesting minimal interference with sintering behavior [38]. Loss of ignition (LOI) values can be attributed to the release of structural water from clay minerals (especially illite and kaolinite), as well as the decomposition of minor carbonates and sulfates. Overall, the chemical composition aligns well with industrial requirements for structural ceramics. The combination of sufficient aluminosilicate content (for strength and plasticity), fluxing oxides (for sintering), and Fe-bearing phases (for red coloration) make these materials viable for environmentally efficient ceramic production. The modest variability among the four samples suggests consistency across the deposit, supporting the use of these schists as a local and sustainable resource for red ceramics.

In the clay schist samples, Ba concentration ranged from 545 to 875 mg/kg (Table 3), a trace element commonly associated with feldspar-rich phases or substitution in phyllosilicates. The high Ba contents are typical of detrital clays and are not expected to significantly impact ceramic properties [39]. Chromium may be derived from associated chloritic phases and, despite not interfering with ceramic processing, it may influence color development depending on firing atmosphere and redox conditions [30]. Nickel and Cu, while not technologically detrimental at the concentrations found, may contribute to post-firing coloration under reducing conditions. The element As showed significant variation, reaching 366 mg/kg in sample 3. Though As is not uncommon in meta-sediments, its elevated concentration may raise concern if the material is used in red ceramics intended for prolonged human contact. Studies have shown that As can leach from both glazed and unglazed ceramic ware, potentially leading to concentrations in food simulants that exceed safety thresholds, e.g., [40]. Çiftçi and Henden [41] revealed that As leached from ceramic foodware can reach levels as high as 1.93–15 mg/L under acidic conditions, above many regulatory limits. Inorganic As is classified as a Group 1 carcinogen by IARC [42] and is associated with a wide spectrum of adverse health effects, including skin and lung cancer, cardiovascular disease, and neurological impairments. Given As risk, the use of sample 3 in ceramic products for food contact should be preceded by rigorous leaching tests (e.g., GB 4806.4 [43] or EN food-contact regulations [44]) and a formal risk assessment. Similarly, given that Pb volatilizes at high temperatures, its concentration must be monitored when materials are intended for glazed or coated ceramic products. The element Zn, despite being in moderate concentration, may contribute positively to glaze coloration, V can influence ceramic color expression, especially under oxidizing firing, while Rb levels reflect its affinity for K-bearing phyllosilicates such as illite and K-feldspar. The Sr values likely reflect Ca-bearing accessory phases like calcite.

Table 3. Trace element concentrations of the clay schist samples (in mg/kg).

ID	As	Ba	Cr	Cu	Nb	Ni	Pb	Rb	Sr	V	Zn	Zr
1	58	711	114	35	22	48	49	141	197	98	175	203
2	83	782	121	31	23	46	23	145	217	90	176	232
3	366	545	133	48	19	62	27	146	120	101	163	160
4	177	875	163	23	28	44	13	231	215	119	151	160

The specific surface area (SSA) values obtained for the four clay schist samples were low and relatively homogeneous, ranging from 2.37 to 2.74 m^2/g (Figure 5). These values are characteristic of clay materials dominated by illite and other non-expanding phyllosilicates, typically exhibiting low SSA, when compared to smectitic clays [45]. Despite the SSA similarity, sample 4 showed the highest expandability (12%), suggesting greater water uptake and volume change upon hydration. This behavior may be attributed to subtle textural or mineralogical differences, such as minor smectitic contributions, not detected in XRD analysis. Expandability is a critical parameter in ceramic processing, particularly for extrusion and drying, as it influences the plasticity, shaping behavior, and shrinkage sensitivity of the clay body. Materials with excessive expansion during wetting may exhibit dimensional instability or cracking during drying, especially if not adequately tempered with non-plastic additives [46]. While the SSA values suggested limited cation exchange or adsorption potential, the moderate expandability of samples 1 to 3 and the higher value for sample 4 may affect water demand and drying kinetics and should be considered in formulation adjustments. From a ceramic standpoint, the combination of low SSA and controlled expandability is favorable for the production of structural ceramics, like bricks and roofing tiles, as it promotes mechanical strength and reduces drying defects. However, materials with higher expandability, such as sample 4, may require blending with more inert materials to optimize dimensional control and avoid warping or cracking during the drying and firing stages [1].



Figure 5. Schist samples' specific surface area (SSA; m^2/g) and expandability (%) results.

The cation exchange capacity (CEC) values determined for the clay schist samples were generally low, ranging from 5.2 to 6.7 meq/100g (Figure 6), which is consistent with the mineralogical dominance of illite and kaolinite. These clay minerals are known to exhibit inherently low CEC compared to smectitic clays, due to the limited interlayer charge and restricted surface activity [45,47]. Sample 3, with the highest CEC (6.7 meq/100g), suggested a higher degree of structural disorder within kaolinite or the presence of minor amounts of more reactive components such as smectite-like interstratifications or amorphous phases [2]. The exchangeable cations K^+, Na^+, Ca^{2+}, and Mg^{2+} showed that the significantly higher Mg^{2+} content in samples 3 and 4 may indicate better substitution in the octahedral layers

or minor contributions from associated carbonate phases (e.g., dolomite). The Na^+ and K^+ suggested that these alkali metals can combine with anions during firing, potentially leading to efflorescence phenomena on the ceramic surface [1]. In ceramic processing, low-CEC clays such as illitic and kaolinitic materials are preferred for stable rheological behavior and reduced ion exchange with additives, contributing to the dimensional control and mechanical integrity of ceramic bodies during drying and firing [48]. However, the presence of exchangeable Mg^{2+} at elevated levels may improve plasticity and workability, since that does not interfere with firing reactions or promote undesirable mineral formation. While low CEC supports the use of these materials in structural ceramics, monitoring soluble Na^+ and K^+ remains essential to prevent surface defects.

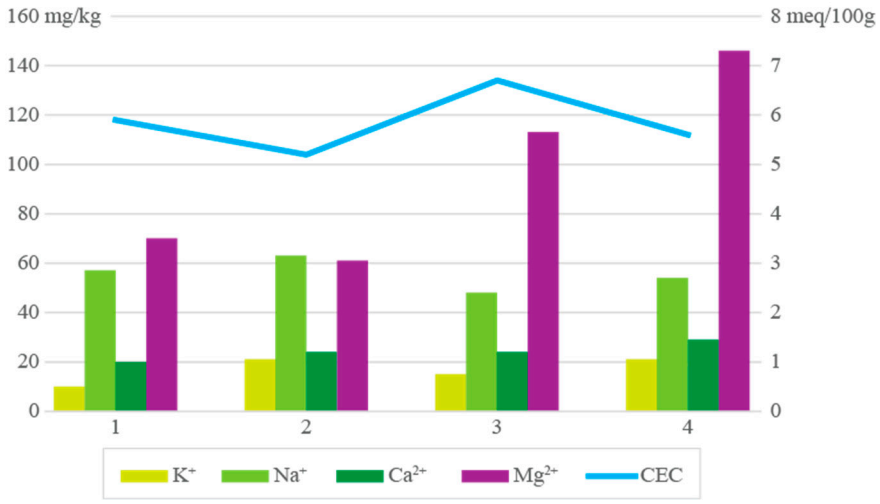


Figure 6. Samples' exchangeable cations, K^+, Na^+, Ca^{2+}, Mg^{2+} (in mg/kg), and cation exchange capacity (CEC; in meq/100g).

The Atterberg limits determined for the four clay schist samples showed consistency with the mineralogical composition dominated by illite and kaolinite. The liquid limit (LL) ranged from 33.6 to 42.8%, while the plastic limit (PL) varied between 23.1 and 30.1% (Figure 7). The plasticity index (PI), reflecting clay's workability and shaping behavior, ranged from 6.8 to 12.7%. To evaluate the shaping suitability of the four-clay schist for ceramic applications, the plasticity index (PI) and plastic limit (PL) values were projected onto the Bain and Highley [49] diagram, widely used to assess the ceramic forming behavior (Figure 8). As shown in the plasticity chart, none of the samples fall within either zone I or zone II. Instead, all four samples were projected outside the defined fields, indicating that these clays exhibit non-ideal plastic behavior for direct extrusion-based shaping. The relatively low plastic limits and moderate plasticity indices place them in a domain of reduced cohesion and marginal workability, consistent with the dominance of illite and kaolinite, minerals known to impart moderate plasticity and low swelling potential. Samples 1 and 2, with PI ~10–11.5 and PL ~23, might be used in structural ceramics if plasticity is adjusted through the addition of more plastic clays or organic binders. Sample 3, with the lowest PI (6.8), may have limited shaping ability and might be better suited for dry pressing rather than extrusion. Sample 4, although presenting the highest PL (30.1), also lies outside the ideal zones, but could be considered with processing adjustments. While these samples are not naturally optimized for plastic forming, they may still be technologically viable for ceramics if blended with more plastic materials to enhance shaping behavior, reduce cracking risk, and improve green strength, an approach commonly recommended in ceramic body formulations [1,45].

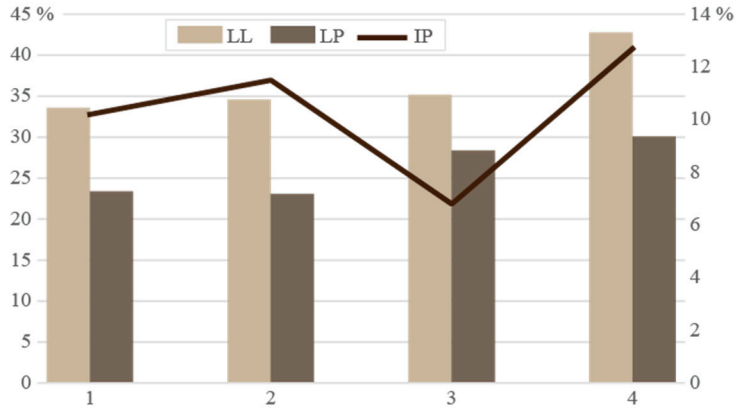


Figure 7. Liquid limit (LL), plastic limit (PL), and plasticity index (PI) of the clay schists.

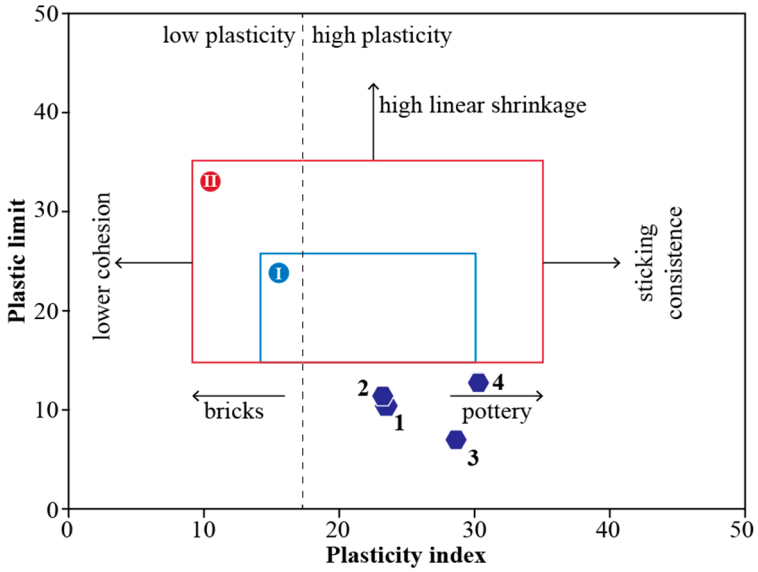


Figure 8. Clay schist samples 1 to 4 projected in the Bain and Highley [49] diagram.

Taking into consideration the previous results, several other assays were performed on a mixture of samples 2 and 3, with a 1:1 proportion. Thermogravimetric analysis (TGA) and differential thermogravimetric analysis (DTG) were performed on a mixture of samples 2 and 3 to assess the thermal behavior and implications for ceramic processing. The resulting curve (Figure 9) revealed four main stages of mass loss, consistent with typical transformations observed in illite- and kaolinite-rich clay materials. In the first stage (up to ~80 °C), a mass loss of approximately 0.93% occurred, corresponding to the evaporation of physically adsorbed water on the surfaces and interlayers of clay minerals. This is characteristic of hydrated phyllosilicates such as illite and minor smectitic phases. The second thermal event occurred between 240.2 °C and 312.5 °C, with a minor mass loss of 0.39%, and may be attributed to the release of loosely bound structural hydroxyl groups. This could reflect disorder within kaolinite or the presence of organic or amorphous components. The main dihydroxylation event begins at 454.7 °C and ends at 717.4 °C, resulting in a 3.27% mass loss. This broader event corresponded to the dihydroxylation of kaolinite (typically 450–600 °C) and illite (600–750 °C), indicating a mineralogical composition dominated by overlapping phases. The broad DTG signal confirmed the complex but expected behavior for mixed-layer clays. Above 800 °C, the mass stabilized, reaching a residual mass of 95.42% at 1120.7 °C. This final stage lacks clear signs of carbonate decomposition, suggesting a low content of thermally unstable carbonates, such as calcite or dolomite. This confirmed earlier mineralogical and chemical findings, supporting a thermally stable ceramic body

formulation. From a technological perspective, overall thermal behavior is favorable for ceramic applications. The low total mass loss (~4.6%) and absence of significant decarbonation suggested a minimal risk of bloating, warping, or unwanted porosity during firing. The predictable dihydroxylation behavior ensures structural transformation and densification suitable for red ceramic products such as bricks and tiles. These findings, combined with prior mineralogical and chemical characterizations, reinforce the suitability of the Barrancos clay schists for structural ceramic production. Their stable thermal profile, moderate dihydroxylation, and minimal carbonate content make them promising candidates for environmentally sustainable ceramic manufacturing.

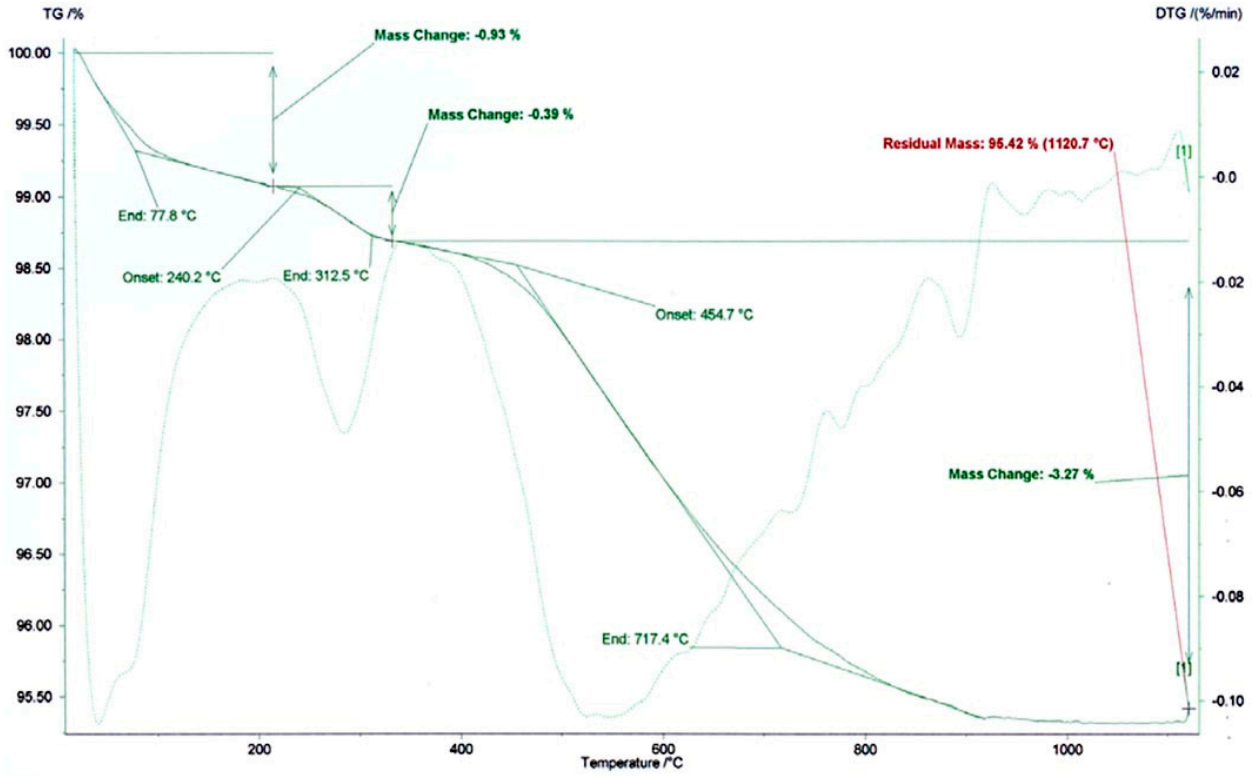


Figure 9. Mixture of clay schists 2 and 3 thermogravimetric analysis (TGA) curve.

Differential scanning calorimetry (DSC) was also performed on the same mixture of samples 2 and 3 to complement the thermal interpretation obtained from TGA. The DSC curve (Figure 10) revealed several endothermic events occurring between room temperature and 1050 °C. The first endothermic signal appeared at ~256 °C, likely associated with the release of weakly bound structural hydroxyl groups or possibly the decomposition of minor organic or amorphous phases. A broad and significant endothermic response was observed between 489 and 662 °C, with inflection points at 489, 578, and 662 °C. These transitions corresponded to the dihydroxylation of kaolinite and illite, confirming the overlapping processes observed in the DTG curve. The intensity and spread of these peaks reinforce the idea of a mixed mineralogical composition with both ordered and disordered phyllosilicate structures. At higher temperatures, ~1005 °C, an additional endothermic effect was noted, which may correspond to the onset of vitrification processes or the formation of new mineral phases such as spinels or feldspathic glasses. This transformation is critical in ceramic processing, as it influences sintering kinetics and final mechanical strength. When interpreted together, the TGA and DSC results demonstrate a consistent thermal profile for the Barrancos clay schist mixture. The combination of low mass loss, stable dihydroxylation, and clear vitrification onset confirmed the material's suitability

for structural ceramic applications. These findings supported previous mineralogical and chemical analyses and reinforced the potential of these raw materials in sustainable ceramic manufacturing.

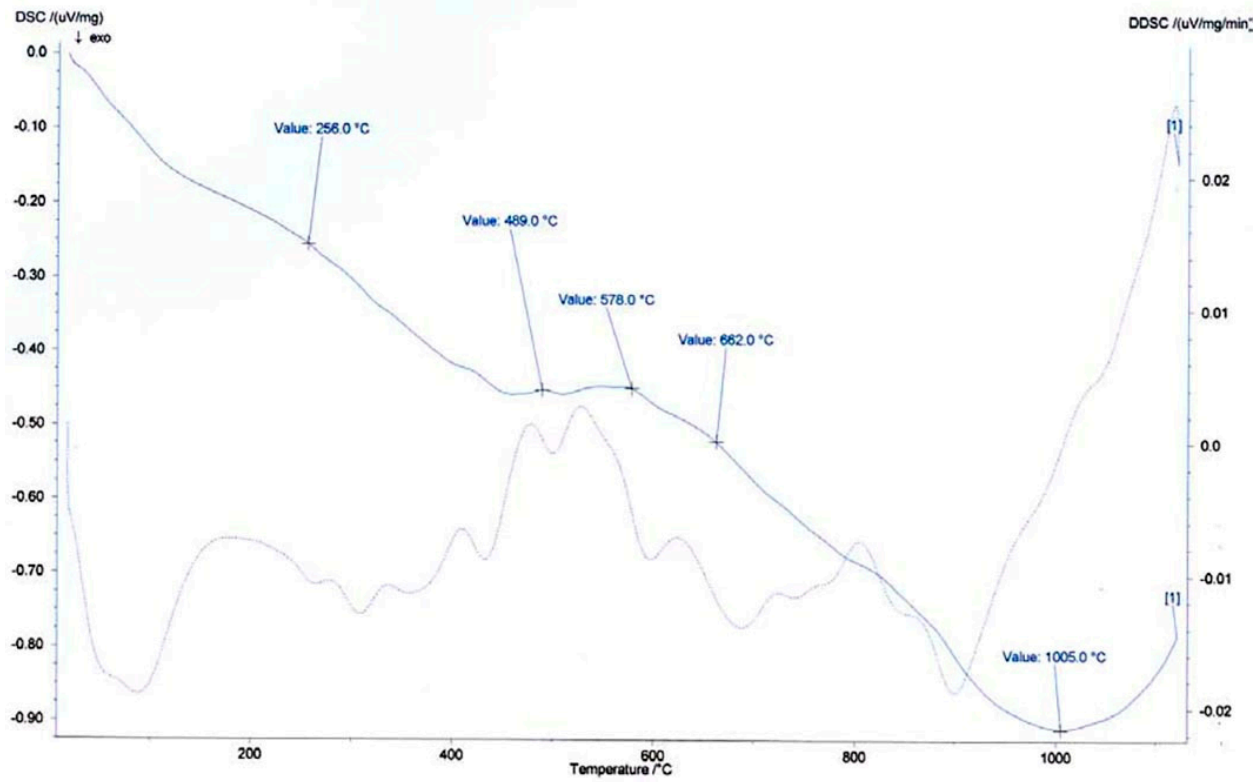


Figure 10. Differential scanning calorimetry curve of the mixture of clay schist 2 and 3 samples.

Thermal dilatometry (TD) was conducted to evaluate the dimensional stability during heating, a key factor for ceramic processing. The dilatometric curve (Figure 11) revealed three distinct phases associated with the material's linear behavior under thermal stress. In the initial stage (ambient to ~600 °C), a slight and continuous linear expansion was observed, typical of the expansion of crystalline lattices as temperature increased, primarily driven by the thermal vibration of atoms within the clay matrix. No abrupt shrinkage or swelling suggested structural integrity and the minimal presence of expansive phases such as smectite. Between ~600 and 1000 °C, the expansion rate increased sharply, indicating the onset of significant phase transformations. This behavior was attributed to the dihydroxylation and partial sintering of clay minerals, particularly illite and kaolinite. The sharpest point of expansion likely reflected the transition toward vitrification, where liquid phase formation begins. Above ~1000 °C, a marked contraction was observed, likely associated with viscous flow and densification during vitrification. This retraction is typical of sintering phenomena in ceramic raw materials, confirming that the material entered the vitrification window. The thermal dilatometric behavior reinforces earlier TGA and DSC interpretations, confirming good thermal compatibility and transformation pathways for ceramic use. The low expansion in early stages and controlled shrinkage in the final stage suggested excellent dimensional control and minimal risk of cracking or warping during firing. This makes the Barrancos clay schists particularly well-suited for red ceramics and structural products such as bricks and roof tiles.

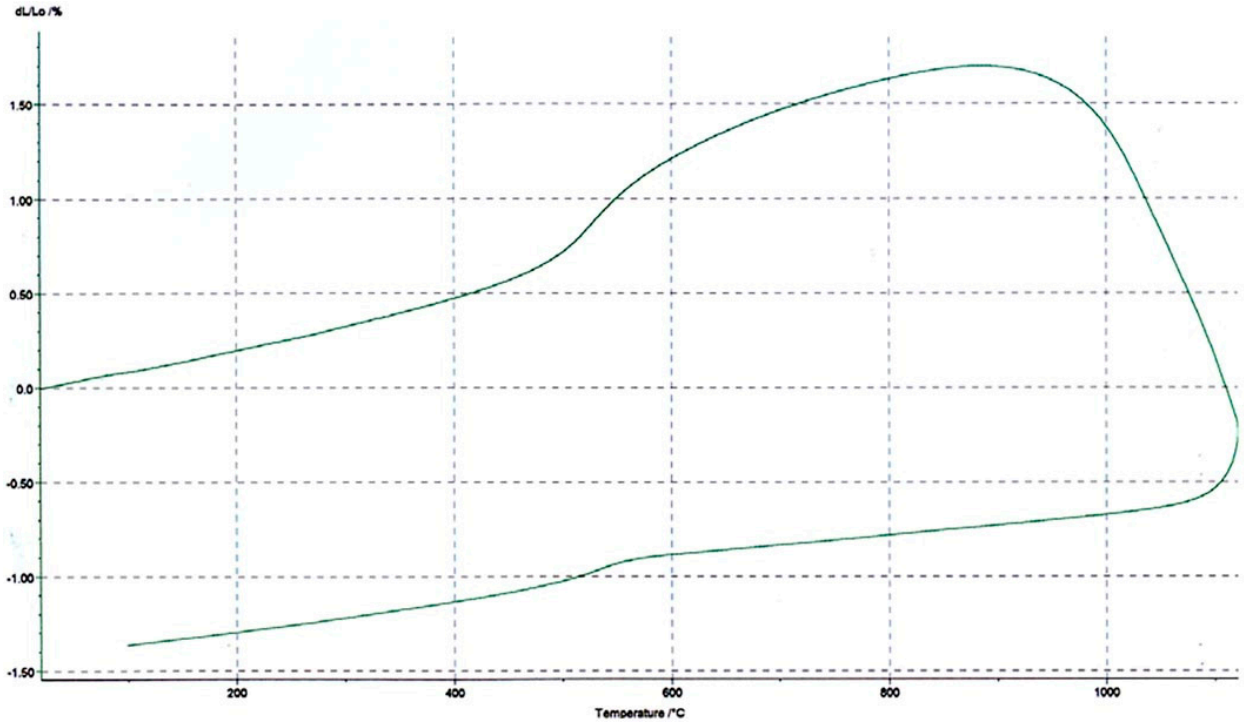


Figure 11. Thermal dilatometry curve of the mixture of clay schist 2 and 3 samples.

The shaping and drying performance of the clay schist mixture (samples 2 and 3) was evaluated through moisture content, linear shrinkage, and flexural strength in the green to dry state. The pressing moisture was 4.5%, indicating adequate plasticity and workability during uniaxial pressing. After drying at 110 °C, the shrinkage from green to dry was limited to 0.25% ± 0.04%, suggesting a dimensionally stable material with a low risk of deformation or cracking during drying. Flexural strength measurements revealed a marked improvement upon drying. The green flexural strength was 3.49 kgf/cm^2, while after drying, it increased to 8.94 ± 0.56 kgf/cm^2, reflecting significant structural consolidation as moisture was removed. The green shrinkage was higher (0.53%) than the final green to dry shrinkage, likely due to elastic recovery and partial relaxation during drying. The combination of low shrinkage and good mechanical performance after drying suggested that the sample mixture exhibited favorable shaping characteristics and good handling properties in the green state. These properties were consistent with ceramic bodies suited for pressing-based forming techniques, where dimensional stability and sufficient green strength are essential for post-forming operations such as machining or handling.

The firing behavior and ceramic properties of the clay schist mixture (samples 2 + 3) after firing in a roller kiln were evaluated at two temperatures (1100 and 1150 °C) (Figures 12 and 13). The total linear shrinkage increased with temperature, from 0.34% ± 0.03% at 1100 °C to 2.13% ± 0.05% at 1150 °C, although it remained relatively low, which is advantageous for controlling dimensional variation during sintering. This moderate shrinkage suggested progressive densification behavior under thermal treatment without inducing excessive contraction. Water absorption decreased markedly with increasing temperature, from 13.34% ± 0.92% to 8.82% ± 0.70%, indicating a significant reduction in open porosity, typical of clay-based ceramics undergoing vitrification, where porosity is closed off as sintering progresses. The densification process was also reflected in the change in color from light orange (1100 °C) to dark orange (1150 °C), consistent with increased Fe^{3+} oxidation and thermal maturation of iron-bearing phases under oxidizing conditions. The flexural strength of the fired specimens increased from 176.52 ± 9.46 kgf/cm^2 at 1100 °C to

282.14 ± 20.33 kgf/cm^2 at 1150 °C, suggesting good mechanical performance. These values indicate that the mixture of clay schist-based ceramic bodies achieved sufficient structural integrity for demanding applications, such as bricks or roofing tiles, even under moderate firing temperatures. Additionally, no efflorescence phenomena were observed on the fired specimens at both temperatures, suggesting that soluble salts such as Na^+ and K^+ were either below critical thresholds or successfully retained within the matrix during firing. This absence enhances the esthetic and durability potential of the final ceramic products. Overall, the results confirm that the sample 2 + 3 mixture showed very good technological behavior upon firing, with progressive sintering, mechanical strength development, and porosity reduction, making it suitable for red ceramic manufacturing in energy-optimized firing regimes.

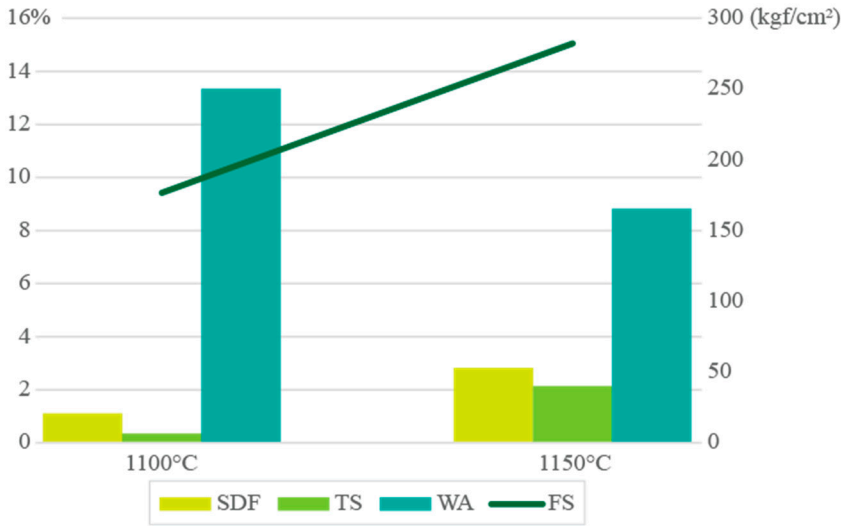


Figure 12. Ceramic properties of schist specimens fired at different temperatures using a 60 min firing cycle of 1100 and 1150 °C, with shrinkage dry-to-fired (SDF; in %); total shrinkage green-to-fired (TS; in %); water absorption (WA; in %); and flexural strength (FS; in kgf/cm^2).

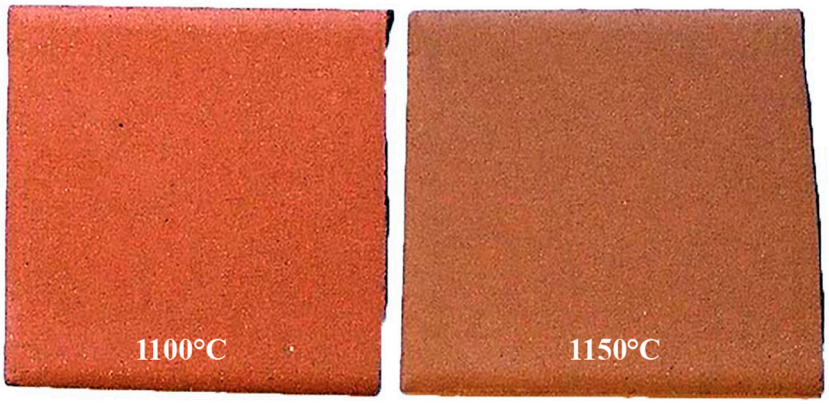


Figure 13. Specimens of mixture of samples 2 and 3 of clay schists, after firing at 1100 and 1150 °C.

The X-ray diffraction patterns of the mixture of clay schist samples 2 and 3, fired at 1100 and 1150 °C (Figure 14), showed that, as expected, clay minerals were the first to disappear upon heating due to dihydroxylation and structural breakdown. In contrast, quartz (SiO_2) and hematite (Fe_2O_3) persisted through the two firing temperatures as stable residual phases. Quartz reflections were clearly identifiable at both temperatures, with their presence suggesting that the heating rate does not significantly influence quartz stability, remaining detectable up to 1150 °C. However, the characteristic quartz peak intensities

progressively decreased with increasing temperature, suggesting partial dissolution and incorporation into the forming glassy matrix during sintering. Hematite was also present at both firing temperatures, showing a slight increase in reflection intensity at 1150 °C, indicating either crystallization from Fe-bearing amorphous phases or increased ordering within the hematite lattice under higher thermal conditions. The most distinctive neo-formed crystalline phase observed was mullite ($3Al_2O_3 \cdot 2SiO_2$), which began to crystallize at 1100 °C, showing a notable increase in reflection intensity at 1150 °C. This phase forms through a solid-state reaction between liberated SiO_2 and Al_2O_3 during firing, marking the onset of ceramic body recrystallization and structural consolidation. The progressive growth of mullite is directly related to the development of mechanical strength and thermal stability in fired ceramics. These mineralogical changes, namely, the absence of clays, the persistence of quartz and hematite, and the formation of mullite, are consistent with sintering dynamics typical of aluminosilicate ceramic systems, confirming the thermal suitability of the studied clay schist mixture for structural ceramic applications.

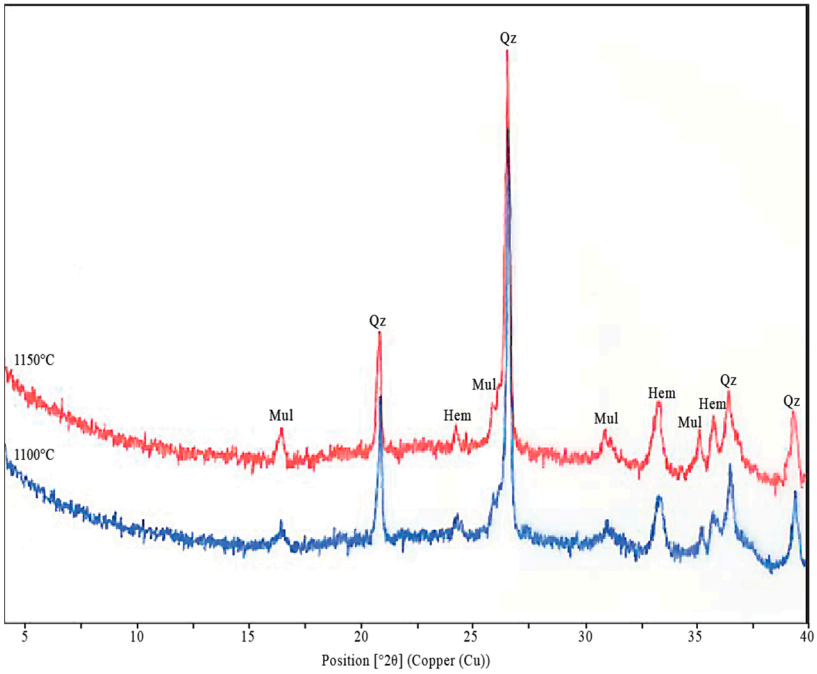


Figure 14. X-ray diffractograms of the mixture of samples 2 and 3 of the clay schists fired at 1100 and 1150 °C. Mul—mullite; Qz—quartz; Hem—hematite.

Barrancos clay schist samples' mineralogical and chemical profiles were consistent with other studies that explored the ceramic potential of schist-derived materials. Mutlu and Mutlu [50] studied the production of ceramic tiles using schist raw materials, highlighting the adequate firing behavior and phase transformations, including mullite formation at high temperatures. Sirbu-Radasanu et al. [51] reported that soils formed from weathered sericite schists in the Eastern Carpathians exhibited illite-rich composition and mineralogical maturity favorable for ceramic applications. These findings aligned with the composition of the Barrancos samples, particularly the Al_2O_3 and SiO_2 content and alkali fluxes (K_2O and Na_2O). Furthermore, Cogswell et al. [52] demonstrated that schist-tempered ceramic pastes used in ancient Hohokam pottery provided both thermal stability and mechanical cohesion. These comparisons reinforce the suitability of Barrancos schists for red ceramic production, particularly when blended or processed to adjust plasticity and granulometric parameters.

4. Conclusions

The clay schists from Barrancos exhibited a mineralogical and granulometric profile that, despite presenting limitations for extrusion in the raw state, demonstrated promising potential for ceramic applications when subjected to simple technological adjustments. The predominance of illite and secondary kaolinite, combined with moderate amounts of quartz, feldspars, and dolomite, ensures a suitable balance between plasticity, thermal stability, and fluxing capacity. Mineralogical and thermal transformations during firing revealed a progressive development of mullite and the persistence of quartz and hematite, corroborating the suitability of these materials for structural ceramics such as bricks and roofing tiles. The low specific surface area, low cation exchange capacity, and moderate expandability further supported the use of these clay schists in controlled ceramic formulations, reducing the risk of deformation or cracking during shaping and drying. Additionally, the samples displayed low heavy metal content, and no efflorescence occurred during firing, suggesting the absence of soluble salts that could compromise esthetics or durability.

Technological tests revealed good ceramic behavior, both before and after firing. Green specimens showed low drying shrinkage and high flexural strength after drying, indicating dimensional stability and robust mechanical performance. Upon firing at 1100 and 1150 °C, the bodies displayed moderate total shrinkage, decreasing water absorption, and high flexural strength. The formation of mullite at 1100 °C, with increasing crystallinity at 1150 °C, was essential for the mechanical consolidation and vitrification of the ceramic matrix. Results confirm that, although the individual samples may not fall within the ideal plasticity domains for extrusion, after blending, they return a technologically viable and sustainable ceramic raw material. From an environmental and economic standpoint, the valorization of these clay schists contributes to the diversification of regional geological resources, offers a low-impact alternative to traditional ceramic clays, and promotes the circular use of materials often considered geotechnical byproducts. Such valorization can support regional development in Barrancos and similar areas, fostering local industries and enhancing the economic utility of sedimentary formations typically overlooked in ceramic manufacturing.

Author Contributions: Methodology, C.C. and F.R.; validation, S.N., C.C., and F.R.; formal analysis, S.N. and C.C.; investigation, C.C., and F.R.; writing—original draft preparation, C.C.; writing—review and editing, C.C. and F.R.; supervision, C.C. and F.R.; funding, F.R. All authors have read and agreed to the published version of the manuscript.

Funding: This work was partially supported by GeoBioTec (UIDB/04035) Research Centre, funded by FEDER funds through the Operational Program Competitiveness Factors COMPETE and by National funds through FCT.

Data Availability Statement: Data will be made available if required.

Conflicts of Interest: The authors declare no conflicts of interest.

References

1. Dondi, M.; Raimondo, M.; Zanelli, C. Clays and bodies for ceramic tiles: Reappraisal and technological classification. *Appl. Clay Sci.* **2014**, *96*, 91–109. [CrossRef]
2. Guggenheim, S.; Martin, R. Definition of Clay and Clay Mineral: Joint Report of the Aipea Nomenclature and CMS Nomenclature Committees. *Clays Clay Min.* **1995**, *43*, 255–256. [CrossRef]
3. Mahmoudi, S.; Bennour, A. Characterisation and ceramic application of clays from North Africa. *Appl. Earth Sci. (Trans. Inst. Min. Metall. B)* **2022**, *31*, 15–26. [CrossRef]
4. Hmeid, H.; Akodad, M.; Baghour, M.; Moumen, A.; Skalli, A.; Azizi, G.; Aalaoul, M.; Gueddari, H.; Daoudi, Y. Preliminary characterization and potential use of different clay materials from North-Eastern Morocco in the ceramic industry. *Mater. Today Proc.* **2022**, *58*, 1277–1284. [CrossRef]

5. Candeias, C.; Santos, I.; Rocha, F. Characterization and Suitability for Ceramics Production of Clays from Bustos, Portugal. *Minerals* **2025**, *15*, 503. [CrossRef]
6. Mezquita, A.; Monfort, A.; Ferrer, S.; Gabaldón-Estevan, D. How to reduce energy and water consumption in the preparation of raw materials for ceramic tile manufacturing: Dry versus wet route. *J. Clean. Prod.* **2017**, *168*, 1566–1570. [CrossRef]
7. Hossain, S.; Roy, P. Sustainable ceramics derived from solid wastes: A review. *J. Asian Ceram. Soc.* **2020**, *8*, 984–1009. [CrossRef]
8. Oliveira, J.; Oliveira, V.; Piçarra, J.M. Traços gerais da evolução tectono-estratigráfica da Zona de Ossa-Morena, em Portugal. *Cad. Lab. Xeolóxico Laxe* **1991**, *16*, 221–250. (In Portuguese)
9. Jensen, S.; Carvalho, C.; Palacios, T. Trace fossils from the Barrancos and Colorada formations, Ordovician, Ossa-Morena Zone, Portugal and Spain. *Comun. Geológicas* **2016**, *103*, 59–168.
10. Robardet, M.; Gutiérrez-Marco, J. The Ordovician, Silurian and Devonian sedimentary rocks of the Ossa-Morena Zone (SW Iberian Peninsula, Spain). *J. Iber. Geol.* **2004**, *30*, 73–92.
11. Novo, S. Caracterização de Xistos Argilosos de Barrancos e Argilas Residuais de S. Pedro do Corval Como Matérias Primas Cerâmicas. Master's Thesis, University of Aveiro, Aveiro, Portugal, 2004. (In Portuguese).
12. Biscaye, P. Mineralogy and Sedimentation of Recent Deep-Sea Clay in the Atlantic Ocean and Adjacent Seas and Oceans. *GSA Bull.* **1965**, *76*, 803–832. [CrossRef]
13. Candeias, C.; Gomes, A.; Rocha, F. Assessment of feldspars from Central Portugal pegmatites for sustainable ceramic applications. *Minerals* **2025**, *15*, 527. [CrossRef]
14. *LNEC E200-67*; Determinação da retração por secagem de argamassas e betões. Laboratório Nacional de Engenharia Civil: Lisboa, Portugal, 1967.
15. *NP 143*; Determinação da Massa Volúmica Aparente e da Porosidade Aparente das Matérias Cerâmicas. Instituto Português da Qualidade: Lisboa, Portugal, 1969. (In Portuguese)
16. Tejeogue, J.; Djakba, R.; Fotsop, C.; Dobe, N.; Mouhamadou, S.; Wangmene, B.; Harouna, M. Systematic metronidazole adsorption performance onto montmorillonite clay: Parametric study, process modelling and RSM optimisation. *Results Chem.* **2025**, *14*, 102153. [CrossRef]
17. *DIN 51006*; Thermal Analysis; Thermogravimetry (TG). General Principles. Beuth Verlag: Berlin, Germany, 1990.
18. *DIN 51007*; Thermal Analysis; Differential Thermal Analysis (DTA). General Principles. Beuth Verlag: Berlin, Germany, 1994.
19. *DIN 51045*; Determination of the Thermal Expansion of Solids—Principles. Beuth Verlag: Berlin, Germany, 1989.
20. Händle, F. *Extrusion in Ceramics*; Springer: Berlin/Heidelberg, Germany, 2009.
21. *ASTM C326-82*; Standard Test Method for Drying and Firing Shrinkages of Ceramic Whiteware Clays. ASTM International: West Conshohocken, PA, USA, 1982.
22. *ASTM C689-97*; Standard Test Method for Thermal Conductivity of Refractory Brick. ASTM International: West Conshohocken, PA, USA, 1997.
23. *EEN 1304*; Clay Roofing Tiles and Fittings—Product Definitions and Specifications. European Committee for Standardization (CEN): Brussels, Belgium, 2013.
24. *N 771-1*; Specification for Masonry Units—Part 1: Clay Masonry Units. European Committee for Standardization (CEN): Brussels, Belgium, 2015.
25. Winkler, V. Bedeutung der Korngrößenverteilung und des Mineralbestandes von Tonen für die Herstellung grobkeramischer Erzeugnisse. *Berichte Der Dtsch. Keram. Ges.* **1954**, *31*, 337–343.
26. Dondi, M. Clay materials for ceramic tiles from the Sassuolo District (Northern Apennines, Italy). Geology, composition and technological properties. *Appl. Clay Sci.* **1999**, *15*, 337–366. [CrossRef]
27. Dondi, M. Feldspathic fluxes for ceramics: Sources, production trends and technological value. *Res. Conserv. Recyc.* **2018**, *133*, 191–205. [CrossRef]
28. Wiśniewska, K.; Pichór, W.; Kłosek-Wawrzyn, E. Impact of the addition of dolomite to cream-firing clays on the technological and color properties of sintered ceramics. *Int. J. Appl. Ceram. Technol.* **2021**, *18*, 1063–1073. [CrossRef]
29. Viani, A.; Cultrone, G.; Sotiriadis, K.; Ševčík, R.; Šašek, P. The use of mineralogical indicators for the assessment of firing temperature in fired-clay bodies. *Appl. Clay Sci.* **2018**, *163*, 108–118. [CrossRef]
30. Bonis, A.; Cultrone, G.; Grifa, C.; Langella, A.; Leone, A.; Mercurio, M.; Morra, V. Different shades of red: The complexity of mineralogical and physicochemical factors influencing the colour of ceramics. *Ceram. Int.* **2017**, *43*, 8065–8074. [CrossRef]
31. MacKenzie, R. Differential Thermal Analysis and its use in Soil—Clay Mineralogy. *Geol. Föreningen I Stockh. Förhandlingar* **1956**, *78*, 508–525. [CrossRef]
32. Kłosek-Wawrzyn, E.; Małolepszy, J.; Murzyn, P. Sintering Behavior of Kaolin with Calcite. *Procedia Eng.* **2013**, *57*, 572–582. [CrossRef]
33. Ouahabi, M.; Daoudi, L.; Hatert, F.; Fagel, N. Modified Mineral Phases During Clay Ceramic Firing. *Clays Clay Min.* **2015**, *63*, 404–413. [CrossRef]

34. Abad, I. Physical meaning and applications of the illite Kübler index. In *Proceedings of the Seminario Sobre, Ineralogía Aplicada*; Universidad de Granada: Granada, Span, 2006; pp. 1–10. (In Spanish)
35. Gomes, C. *Argilas, o Que São e Para Que Servem*; Fundação Calouste Gulbenkian: Lisboa, Portugal, 1988. (In Portuguese)
36. Ferrari, S.; Gualtieri, A. The use of illitic clays in the production of stoneware tile ceramics. *Appl. Clay Sci.* **2006**, *32*, 73–81. [CrossRef]
37. Pavlova, I.; Sapozhnikova, M.; Farafontova, E. The Effect of Manganese-Containing Pigment on the Strength of Ceramic Bricks. *Mater. Sci. Forum* **2020**, *989*, 329–334. [CrossRef]
38. Bianchini, G.; Marrocchino, M.; Moretti, A.; Vaccaro, C. Chemical-mineralogical characterisation of historical bricks from Ferrara: An integrated bulk and micro analytical approach. *Lond. Geol. Soc. Spec. Publ.* **2006**, *257*, 127–139. [CrossRef]
39. Reitz, A.; Pfeifer, K.; Lange, G.; Klump, J. Biogenic barium and the detrital Ba/Al ratio: A comparison of their direct and indirect determination. *Mar. Geo.* **2004**, *204*, 289–300. [CrossRef]
40. Henden, E.; Cataloglu, R.; Aksuner, N. Determination of arsenic leaching from glazed and non-glazed Turkish traditional earthenware. *Sci. Total Environ.* **2011**, *409*, 2993–2996. [CrossRef]
41. Çiftçi, T.; Henden, E. Leaching of arsenic from glazed and nonglazed potteries into foods. *Sci. Total Environ.* **2016**, *569–570*, 1530–1535. [CrossRef]
42. IARC. Arsenic, Metals, Fibres and Dusts. A Review of Human Carcinogens. In *IARC Monographs on the Evaluation of Carcinogenic Risks to Humans*; International Agency for Research on Cancer: Lyon, France, 2012; Volume 100C.
43. *GB 4806.4*; National Food Safety Standard—Ceramics for Food Contact. National Health and Family Planning Commission of China and Standardization Administration of China: Beijing, China, 2016.
44. European Union. EC1935/2004 of the European Parliament and of the Council of 27 October 2004 on materials and articles intended to come into contact with food and repealing Directives 80/590/EEC and 89/109/EEC. *Off. J. Eur. Union.* **2004**, *L338*, 4–17.
45. Murray, H. *Applied Clay Mineralogy: Occurrences, Processing and Applications of Kaolins, Bentonites, Palygorskite, Sepiolite, and Common Clays*; Elsevier: Amsterdam, The Netherlands, 2006.
46. Grim, R.E. Clay mineralogy. In *International Series in the Earth and Planetary Sciences*, 2nd ed.; McGraw Hill: Columbus, OH, USA, 1968.
47. Bergaya, F.; Lagaly, G. *Handbook of Clay*; Elsevier: Amsterdam, The Netherlands, 2013.
48. Carty, W.; Senapati, U. Porcelain—Raw Materials, Processing, Phase Evolution, and Mechanical Behavior. *J. Am. Ceram. Soc.* **2005**, *81*, 3–20. [CrossRef]
49. Bain, J.; Highley, D. Regional appraisal of clay resources: A challenge to the clay mineralogist. *Dev. Sedimentol.* **1966**, *27*, 437–447.
50. Mutlu, H.; Mutlu, A. Analysis of tiles produced from a schist material and their ultraviolet, near-infrared, mid-infrared, longwave-infrared and far-infrared spectra. *Clay Miner.* **2022**, *56*, 292–298. [CrossRef]
51. Sirbu-Radasanu, D.S.; Huzum, R.; Dumitraş, D.-G.; Stan, C.O. Mineralogical and geochemical implications of weathering processes responsible for soil generation in Mănăila Alpine Area (Tulgheş 3 Unit—Eastern Carpathians). *Minerals* **2022**, *12*, 1161. [CrossRef]
52. Cogswell, J.; Abbott, D.; Miska, E.; Neff, H.; Speakman, R.; Glascock, M. A Provenance study of Hohokam schist-tempered pottery and raw materials from the Middle Gila River Valley, Arizona: Techniques and prospects. In *Laser Ablation ICP-MS in Archaeology*; Speakman, R.J., Neff, H., Eds.; University of New Mexico Press: Albuquerque, NM, USA, 2005; pp. 105–115.

Disclaimer/Publisher's Note: The statements, opinions and data contained in all publications are solely those of the individual author(s) and contributor(s) and not of MDPI and/or the editor(s). MDPI and/or the editor(s) disclaim responsibility for any injury to people or property resulting from any ideas, methods, instructions or products referred to in the content.